VIRTUAL CRANIOFACIAL RECONSTRUCTION FROM COMPUTED TOMOGRAPHY IMAGE SEQUENCES EXHIBITING MULTIPLE FRACTURES

A.S. Chowdhury[1], S.M. Bhandarkar[1], R.W. Robinson[1], J.C. Yu[2]
{ananda@cs.uga.edu, suchi@cs.uga.edu, rwr@cs.uga.edu, jyu@mcg.edu}

[1]Department of Computer Science
The University of Georgia
Athens, GA 30602-7404, USA.

[2]Department of Plastic Surgery
The Medical College of Georgia
Augusta, GA 30912-4080, USA.

ABSTRACT

A novel procedure for in-silico (virtual) craniofacial reconstruction of human mandibles with multiple fractures from a sequence of Computed Tomography (CT) images is presented. The problem is formulated as one of combinatorial pattern matching and solved in two stages. First, the opposable fracture surfaces are identified using a maximum weight graph matching algorithm where the fracture surfaces are modeled as the vertices of a weighted graph. The edge weights between pairs of vertices are treated as elements of a score matrix, whose values are a linear combination of (a) the Hausdorff distance, and (b) a score function based on fracture surface characteristics. Second, the pairs of opposable fracture surfaces identified in the first stage are actually registered using the Iterative Closest Point (ICP) algorithm enhanced with a graph theoretic improvisation. The correctness of the registration in the second stage is constantly monitored by volumetric matching of the reconstructed mandible with an intact mandible. Experimental results on simulated CT image sequences of broken human mandibles are presented.

Keywords: Biomedical image processing, Image registration, Graph theory, Pattern matching.

1. INTRODUCTION

Craniofacial fractures are very frequently encountered in modern society with the major causes being vehicle accidents, sports-related injuries and gunshot wounds [1]. The issue of *virtual* surgical reconstruction is critical even in a single-fracture instance as the surgeon needs to precisely, and in an expeditious manner, register the two bone fragments, thereby preventing any possible misalignment between them. The problem is far more complex in case of multiple fractures [2] and the cost of surgery becomes prohibitive with the increased operative time necessary to identify accurately the opposable fracture surfaces and thereby ensure an overall accurate reconstruction [3]. The reconstruction problem is essentially combinatorial in nature and hence is a topic of general interest in other problems such as jigsaw puzzle solving [4-5] and broken earthenware assembly [6]. The present paper provides a novel two step solution to the virtual multi-fracture reconstruction problem, which can be easily extended to similar problems in other domains. In the first step, the opposable fracture surfaces are identified using the maximum weight graph matching algorithm for a weighted graph, and a pre-computed score matrix. In the second step, the opposable fracture surface pairs identified in the first step are registered using an improvised ICP algorithm, where the closest set is determined using the maximum cardinality minimum weight bipartite graph matching algorithm. The reconstruction process in the second step is constantly monitored using two simple but useful constraints based on the Tanimoto coefficient and concepts of volumetric matching.

2. FORMULATION OF THE SCORE MATRIX

The input to the reconstruction procedure is a sequence of CT images of the fractured human mandible. A score matrix is constructed based on the appearance of various mandible fragments in the input CT image sequence. The mandible fragments are classified as terminal or non-terminal, based on the presence or absence of condyles (a craniofacial body part that exhibits pronounced sphericity) respectively. For simplicity, we currently assume that a terminal fragment can have a singe fracture surface whereas a non-terminal fragment can have two fracture surfaces. However, our scheme is flexible enough to handle any number of fracture surfaces for a given fragment. Each fracture surface is represented by a collection of 3D data points obtained by extracting and collating the corresponding fracture contour points in the 2D CT image slices. In the case of 2D problems, the score matrix formulation is typically based on curve matching [4], where the matrix elements denote matches between potentially opposable edge points [7]. In our case, we need to estimate the matching score between the 3D fracture surfaces extracted from the CT image slices. A high matching score is assigned to a pair of fracture surfaces if (a) they are determined to be spatially proximal, and (b) they are determined to exhibit complementary (opposable) fracture surface characteristics. We have used both of these factors in determining the matching score.

2.1. Mathematical Formulation of Spatial Proximity

Since the various fracture surfaces possess a varying number of data points, the notion of a distance (as a measure of spatial separation) between any surface pair requires the establishment of correspondence between the data points, which is computationally very expensive. We therefore use the Hausdorff distance, since it does not need a prior correspondence between the two data point sets to give a measure of spatial separation between them. The Hausdorff distance *H(A, B)* between two data sets A and B is given by [8]:

$$H(A,B) = \max(h(A,B), h(B,A)) \quad (1)$$

where *h(A, B)* denotes the *directed* Hausdorff distance between the two data sets A and B defined by

$$h(A,B) = \max_{a \in A} \min_{b \in B} \|a - b\| . \quad (2)$$

Here ||*a* - *b*|| represents the Euclidean distance between the points *a* and *b*. Each such *a, b* in our case is a 3D data point in the fracture surface data set *A* and *B* respectively. The computation of the Hausdorff distance can be done in *O(mn)* time where *m* and *n* denote the cardinalities of the two fracture surface data sets.

2.2. Mathematical Formulation of Surface Characteristics

Each fracture surface is essentially a collection of several fracture contours. For each surface, we maintain an ordering of the contour curvature extracted from the various CT image slices constituting the fracture surface. The choice of contour curvature as a measure of surface irregularity is guided by the fact that it enjoys rotational and translational invariance. The contour curvature for a point *(x, y)* in a given CT image slice (for a specific value of *z*) is given by [9]:

$$c(x,y) = \frac{d^2y}{dx^2} \Big/ (1 + (\frac{dy}{dx})^2)^{3/2} \quad (3)$$

A score function *FS(A, B)* for a pair of fracture surfaces *A* and *B* is the sum of the score *fs(a, b)* for each possible point pair, one from each surface. If the two points under consideration have the same signs for their curvatures, then they cause the overall score for the surface to increase; otherwise they cause it to decrease. The score function is formally given by:

$$FS(A,B) = \sum_{a \in A} \sum_{b \in B} fs(a,b) \quad (4)$$

The score *fs(a,b)* between a pair of points *a* and *b* is high if (a) the slice-wise locations of two points are spatially proximal, and (b) the relative positions/enumeration values of the two points in respective slices (estimated using the end-points of the slices as the reference points) are close and (c) the curvature values of the two points are close. The score will be low if any of the above criteria are not satisfied. Mathematically *fs(a, b)* is the product of the above three factors and a sign factor, as follows:

$$fs(a,b) = S(a,b)E(a,b)C(a,b)sg(c_a c_b) , \quad (5)$$

where $$S(a,b) = 2/(1 + \exp(|s_a - s_b|)) , \quad (6)$$

$$E(a,b) = 2/(1 + \exp(|e_a - e_b|)) , \quad (7)$$

$$C(a,b) = 2/(1 + \exp(|c_a - c_b|)) . \quad (8)$$

Here *S(a, b)*, *E(a, b)* and *C(a, b)* respectively denote the slice-wise, enumeration value-wise and curvature value-wise scores of the two points *a* and *b* and s_a (s_b), e_a (e_b), c_a (c_b) respectively denote the slice value (*i.e. z*-value), enumeration value of the point in the slice and contour curvature value (given by eqn. (3)) of the point *a* (*b*). Also, *sg(x)* is the sign function, such that *sg(x)*=1 if $x > 0$, *sg(x)*=0 if $x = 0$, and *sg(x)*=-1 if $x < 0$. Each of the functions in eqns. (6), (7) and (8) is designed to capture the prominent variations of the corresponding component terms. Each term has an absolute value in the interval [0, 1], and thus constitutes a fuzzy function, except for the sign.

2.3. Score Matrix Elements

The score *SC(A, B)* between two surfaces *A* and *B* is a linear combination of the inverse of the Hausdorff distance (from eqn. (1)) and the surface matching score (from eqn. (4)):

$$SC(A,B) = \lambda_1 H^{-1}(A,B) + \lambda_2 FS(A,B) \quad (9)$$

The smaller the Hausdorff distance (*i.e.*, the greater the inverse value), the greater the possibility of the surfaces being opposable. Similarly, the greater the surface matching score value, the greater the possibility of the surfaces being opposable. The coefficients of linear combination are determined using following equations:

$$\lambda_1 + \lambda_2 = 1 \quad (10)$$

$$\frac{\lambda_1}{\sigma(H^{-1}(A,B))} = \frac{\lambda_2}{\sigma(FS(A,B))} = \frac{1}{\sigma(H^{-1}(A,B)) + \sigma(FS(A,B))} \quad (11)$$

In eqn. (11), $\sigma(H^{-1}(A, B))$ and $\sigma(FS(A, B))$ respectively denote the standard deviation of $H^{-1}(A, B)$ and *FS(A, B)* for all possible fracture surface pairs *A* and *B*. With the incorporation of the Euclidean distance in eqn. (2), the Hausdorff distance in eqn. (1) can correctly represent the spatial proximity of two fracture surfaces that have undergone rigid body motion [8]. Furthermore, the use of contour curvature, a rigid body motion invariant feature [9], allows the score matrix to correctly handle relative rotation and translation amongst the various fracture surfaces.

3. COMBINATORIAL PATTERN MATCHING

In this section, we first show that our multi-fracture reconstruction problem results in a combinatorial explosion in terms of number of possible reconstruction options. The maximum weight graph matching algorithm is presented next as a novel solution to this problem.

3.1. Combinatorial Nature of the Reconstruction Problem

Theorem: *Given that a non-terminal fragment has two fracture surfaces and a terminal fragment has one fracture surface, the number of possible reconstruction options* rc_n *where n is the total number of fragments is:*

$$rc_n = (n-2)!2^{n-2} \quad (12)$$

Proof: With *n* total fragments, the $n-2$ non-terminal fragments can be encountered in any of $(n-2)!$ possible orderings. Further, each non-terminal fragment can be oriented such that either of the fracture surfaces is the first in the sequence. This accounts for the factor 2^{n-2} in counting the possibilities. It is clear from eqn. (12) that the problem leads to a combinatorial explosion [10].

3.2. Solution to the Combinatorial Reconstruction Problem

The combinatorial reconstruction problem is usually formulated as a Traveling Salesman Problem (TSP) [4]. However, the TSP by itself is an NP-hard problem [10], *i.e.*, determining the optimal solution to the TSP entails a factorial-time algorithm in the worst case. Instead, we model the reconstruction problem as a Maximum Weight Graph Matching (MWGM) problem for a weighted graph [11], where the fracture surfaces are modeled as the vertices of a weighted graph *G* and the entries of the score matrix are assigned the edge weights between the corresponding vertices. The MWGM algorithm for a non-bipartite graph has a polynomial time complexity of $O(n^4)$, where *n* is the number of vertices [11]. We obtain the *k* best solutions, where $k \geq 2$ and the solutions are indexed by *j* (*j* = 1…*k*). Each solution is a set of unordered opposable fracture surface pairs. Let W_j denote the sum of the edge-weights for the current best solution and W_{j+1} denote the sum of the edge-weights for the next best solution. Successive solutions are generated until the following condition is violated:

$$W_j - W_{j+1} < pW_j . \quad (13)$$

where *p* is an appropriately chosen positive fraction.

4. FRACTURE SURFACE REGISTRATION

The fracture surface pairs are accurately registered using an improvised Iterative Closest Point (ICP) algorithm [12] in the second step of the overall reconstruction problem. The main steps in the improvised ICP algorithm are described below [13]:

(a) The matching points in one fracture surface data set, called the model data set, corresponding to points in the other fracture surface data set, called the sample data set, are determined and termed the *closest set.* The matching point pairs are determined using the Maximum Cardinality Minimum Weight (MCMW) matching algorithm for a bipartite graph [11, 14]. The use of the MCMW graph matching algorithm obviates the need for any prior alignment of the two fracture surface data sets. The sample and model data sets correspond to the two disjoint vertex sets V_1 and V_2 (with potentially different cardinalities) respectively in the bipartite graph $G_B(V_1 \cup V_2, E)$. The edge-weight $(W_{ij} \in E)$ between any two nodes i and j (such that $i \in V_1$ and $j \in V_2$) is deemed to be the Euclidean distance between them. Note that the Euclidean distance is invariant under a 3D rigid body transformation. Thus, the edge weights are given by:

$$W_{ij} = [(x_i - x_j)^2 + (y_i - y_j)^2 + (z_i - z_j)^2]^{1/2} \quad (14)$$

(b) The computed transformation is applied to the original sample data set and the Mean Squared Error (MSE) between the transformed sample data points and the corresponding closest points is computed. The MSE (ε^2) is given by:

$$\varepsilon^2 = (1/N)\sum_{i=1}^{N} \left\| c_i - (Rs_i + T) \right\|^2 \quad (15)$$

where R denotes the rotation matrix, T the translation vector, s_i a point of the sample data set and c_i the corresponding point in the closest set. Steps (a)-(b) are repeated with an updated sample set (generated by applying R and T obtained at the current iteration to the current sample set) until a pre-specified error convergence criterion (0.001 in our case) is reached.

5. GLOBAL SHAPE MONITORING

As mentioned in Section 3, the k best possible solution sets are obtained from the MWGM algorithm. The actual registration of the fracture surface pairs is done with the best solution set (using the ICP algorithm). After each pair of fracture surfaces are registered, the global shape of the partially reconstructed mandible is monitored using a measure of volumetric overlap with the unbroken reference mandible. In the context of volumetric matching, the Tanimoto coefficient $TC_{f,g}$ between two volumetric shapes f and g is defined as [15]:

$$TC_{f,g} = \frac{O_{f,g}}{I_f + I_g - O_{f,g}} \quad (16)$$

where

$$I_f = \iiint f^2(\hat{x},\hat{y},\hat{z})dv \quad (17)$$

$$I_g = \iiint g^2(\tilde{x},\tilde{y},\tilde{z})dv \quad (18)$$

$$O_{f,g} = 2\iiint f(\hat{x},\hat{y},\hat{z})g(\tilde{x},\tilde{y},\tilde{z})dv \quad (19)$$

Here $(\hat{x},\hat{y},\hat{z}) = (x - x_{RC}, y - y_{RC}, z - z_{RC})$, where (x_{RC}, y_{RC}, z_{RC}) is the centroid of the reference mandible R. Similarly, $(\tilde{x},\tilde{y},\tilde{z}) = (x - x_{SC}, y - y_{SC}, z - z_{SC})$, where (x_{SC}, y_{SC}, z_{SC}) is the centroid of the reconstructed mandible S. Then, we have:

$$f(\hat{x},\hat{y},\hat{z}) = \begin{cases} 1 & if\ (\hat{x},\hat{y},\hat{z}) \in R \\ 0 & otherwise \end{cases} \quad (20)$$

$$g(\tilde{x},\tilde{y},\tilde{z}) = \begin{cases} 1 & if\ (\tilde{x},\tilde{y},\tilde{z}) \in S \\ 0 & otherwise \end{cases} \quad (21)$$

Now, we introduce two volumetric matching-based shape constraints for the purpose of monitoring the global correctness of the reconstruction:

i) With the registration of each fracture surface pair, the value of the $TC_{f,g}$ should be monotonically non-decreasing.

ii) In the present reconstruction scenario, since S is a subset of R, ideally, the overlapped volume $O_{f,g}$ at each stage should be exactly twice the volume of the partially reconstructed mandible I_g. This can be seen from eqns. (17) – (19) with the fact that the volume of the reference mandible I_f always remains constant. We then define the correctness criterion as

$$(2I_g - O_{f,g}) \le (2qI_g) \quad (22)$$

where q is an appropriately chosen positive fraction. At any point in the reconstruction stage if either of the two constraints is violated, we abandon the current solution and restart the registration with the next best solution of the MWGM algorithm.

6. EXPERIMENTAL RESULTS

Experimental results are restricted to a single (multi-fracture) case to conserve space. The input CT image sequence has six broken human mandible fragments with a total of ten fracture surfaces. The two fracture surfaces belonging to the terminal fragments are numbered 1 and 10 and the remaining eight fracture surfaces of the non-terminal fragments are numbered from 2 to 9.

TABLE 1. Extreme Score Parameter values

Score Parameter Extremes	Value	Fracture Surface Pair
Min. Hausdorff distance	29.83	(5, 6)
Max. Hausdorff distance	185.12	(1, 9)
Min. Surface Match	-413.39	(4, 9)
Max. Surface Match	955.55	(1, 4)
Min. Overall Score	1	(4, 9)
Max. Overall Score	1362	(1, 4)

TABLE 1 shows the extreme values of the Hausdorff distance, the surface match function and the overall score amongst all possible fracture surface pairs. The surface match values are normalized so that the minimum value is 1.0 before using them in eqn. (9) to ensure all positive weights for the graph. The overall score elements are also rounded to their nearest integer values for the graph matching algorithm. For the present CT image sequence, the surface match clearly dominates the overall score. However, for a different CT image sequence with fairly similar fracture surface characteristics, the spatial proximity of the fracture surfaces could easily be more decisive. This justifies the inclusion of the Hausdorff distance term in the overall score.

TABLE 2. Results from the Graph Matching Algorithm

Solution Set (j)	W_j
{(1,4), (2, 5), (3, 6), (7, 8), (9, 10)}	4987
{(1,3), (2, 9), (4, 6), (5, 7), (8, 10)}	3123

TABLE 2 shows the solution set obtained from the MWGM algorithm along with the sum of the edge weights for each solution set. We chose p = 0.1, which in this case led to termination after obtaining two best solution sets based on eqn. (13).

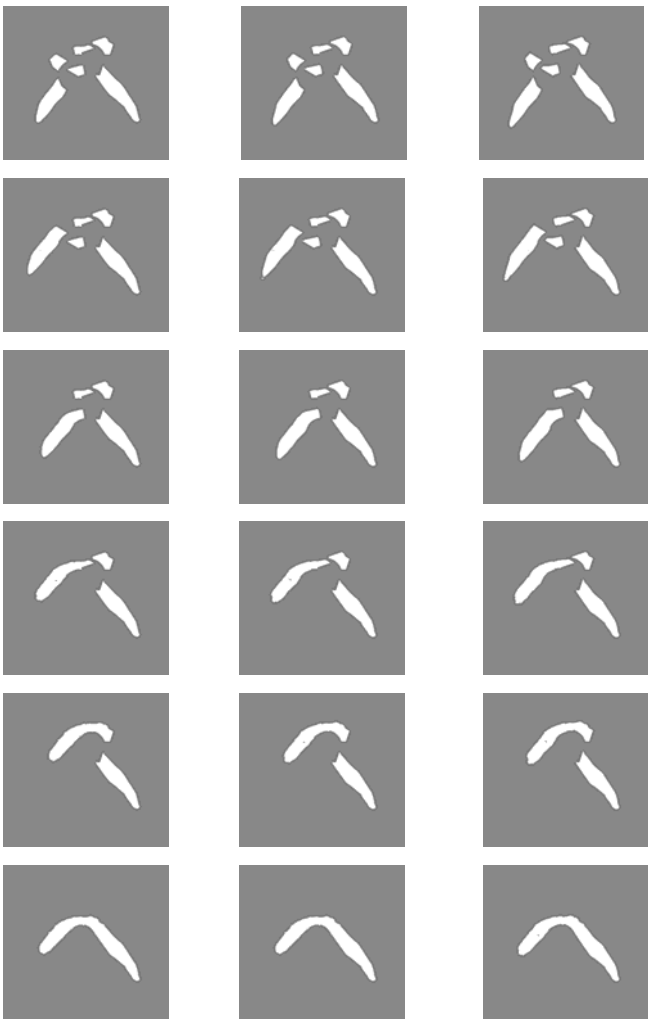

Fig. 1. Different Stages of Mandibular Reconstruction

Fig. 1 describes the various stages of the reconstruction with the best solution set (obtained from row 1 of Table 2) using the improvised ICP algorithm described in Section 4. The first row shows three successive images in the original CT sequence with six broken fragments or components (denoted by bright intensity values), obtained after preprocessing the original CT image sequence. Each of the later five rows shows the same three images with a new pair of fracture surfaces registered at each stage.

TABLE 3. Results of Shape Monitoring ($A = (2I_g - O_{f,g})/ 2 I_g$)

Various Stages of Reconstruction	$TC_{f,g}$	A
(1, 4) registered	1.08	0
{(1, 4), (2, 5)} registered	1.47	0
{(1, 4), (2, 5), (3, 6)} registered	1.57	0
{(1,4), (2,5), (3,6), (7, 8)} registered	1.69	0
All 5 fracture surface pairs registered	21.71	0.0003

TABLE 3 describes the results of the step-by-step shape monitoring of the partially reconstructed mandible at various stages of reconstruction. At each stage, both shape constraints (defined in Section 5) are satisfied with a choice of $q = 0.01$. Thus, we proceed with the best solution of the MWGM algorithm to complete the registration of all five fracture surface pairs.

7. CONCLUSIONS AND FUTURE RESEARCH

The paper addresses an extremely challenging biomedical imaging problem, *i.e.*, that of multi-fracture craniofacial reconstruction. The problem is cast as one of combinatorial optimization for which a novel, general and efficient solution is proposed. The proposed solution has the potential to considerably reduce the operative time, operative costs and patient trauma during actual craniofacial surgery and also ensure accurate reconstructive surgery. Future research will focus on the use of deformable models, instead of pure volumetric matching, for global shape monitoring [16].

8. REFERENCES

[1] R.E. King, J.M. Scianna and G.J. Petruzzelli, Mandible fracture patterns: a suburban trauma center experience, *Amer. J. Otolaryngology,* 25(5), pp. 301-307, 2004.

[2] B.O. Ogundare, A. Bonnick and N. Bayley, Pattern of mandibular fractures in an urban major trauma center, *J. Oral Maxillofacial Surg.* 61(6), pp. 713-718, 2003.

[3] C. Zahl, D. Muller, S. Felder and K.L. Gerlach, Cost of miniplate osteosynthesis for treatment of mandibular fractures: a prospective evaluation, *Gesundheitswesen,* 65(10), pp. 561-565, 2003.

[4] H. Wolfson, E. Schonberg, A. Kalvin and Y. Lamdan, Solving Jigsaw Puzzles by Computer, *Ann. Oper. Res.*, 12. pp. 51-64. 1988.

[5] D. Goldberg, C. Malon and M. Bern, A Global Approach to Automatic Solution of Jigsaw Puzzles, *Computational Geometry – Theory and Appl.* 28(3), pp. 165-174. 2004.

[6] A. Willis and D. Cooper, Bayesian Assembly of 3D Axially Symmetric Shapes from Fragments, *Proc. IEEE Conf. CVPR,* Washington D.C., USA, pp. 82 – 89, 2004.

[7] J.T. Schwartz and M. Sharir, Identification of partially obscured objects in two dimensions by matching of noisy characteristic curves, *Intl. J. Robotics Res.* 6(2), pp. 29 – 44, 1987.

[8] D.P. Huttenlocher, G.A. Klanderman and W.J. Rucklidge, Comparing Images Using the Hausdorff Distance, *IEEE Trans. PAMI,* 15(9), 850 – 863, 1993.

[9] L.F. Costa and R.M. Cesar Jr., *Shape Analysis and Classification, Theory and Practice,* CRC Press, 2000.

[10] C.H. Papadimitriou and K. Steiglitz, *Combinatorial Optimization, Algorithms and Complexity,* Dover Publications, 1998.

[11] N. Christofides, *Graph Theory: An Algorithmic Approach.* Academic Press, 1975.

[12] P.J. Besl and N.D. McKay, A Method for Registration of 3-D Shapes, *IEEE Trans. PAMI,* Vol. 14(2), pp. 239 – 256, 1992.

[13] S.M. Bhandarkar, A.S. Chowdhury, Y. Tang, J. Yu and E.W. Tollner, Surface Matching Algorithms for Computer Aided Reconstructive Plastic Surgery: *Proc. IEEE ISBI*, pp. 740 – 743, Arlington, VA, USA, 2004.

[14] H.W. Kuhn, "The Hungarian method for the assignment problem," *Nav. Res. Log.* Quart. 2, 1955.

[15] E.J. Mills and P.M. Dean, Three-dimensional hydrogen-bond geometry and probability information from a crystal survey, *Jour. Comput-Aided Mol. Des.*, 10(6), pp. 607 -622, 1996.

[16] T. McInerney and D. Terzopoulos, Deformable Models in Medical Image Analysis: A Survey, *Medical Image Analysis*, 1(2), pp. 91 – 108, 1996.